Stereoregular Polyelectrolyte/Surfactant Stoichiometric Complexes

Jean-Michel Guenet

Institut Charles Sadron, CNRS UPR22, 6 rue Boussingault F-67083 Strasbourg Cedex, France
E-mail guenet@ics.u-strasbg.fr

Summary: The molecular structure of polystyrene sulphonate/CTAB stoichiometric complexes has been studied by small angle neutron scattering in solutions and in gels for *atactic* and *isotactic* conformers of the polystyrene moiety. It is found that tacticity has no influence on the molecular structure in solution but plays a role in the gel state.

Keywords: complex; polyelectrolyte; surfactant; tacticity

Introduction

Natural or synthetic polyelectrolytes can be complexed in aqueous solutions by ionic surfactants through electrostatic interaction between the oppositely-charged sites of both constituents [1-4]. Under stoichiometric conditions, the resulting complex is no longer soluble in water but becomes soluble in organic solvents. Curiously enough, these complexes are soluble in alcohol, such as n-butanol or ethanol, so that they cannot be compared to comb-like polymers with short side-chains. In table 1 is shown the behaviour for a few solvents as a function of the dielectric constant ϵ. As can be seen the solubility range seems to be narrow enough as far as ϵ is concerned. Also, some polyelectrolyte-like behaviour is seen at low concentration of alcohol[3], although any dissociation process as occurs for polylectrolytes in water seems hard to accept in ethanol (see figure 1).

Table 1. Solubility of polylectrolyte/CTAB systems for some solvents vs dielectric constant ϵ.

	ϵ	solubility
decahydronaphthalene	2.2	insoluble
butanol	17.8	soluble
ethanol	25.3	soluble
nitrobenzene	22.9	gels
DMSO	47.2	Phase separates at room temperature
water	80	insoluble

 DOI: 10.1002/masy.200550402

From these alcoholic solutions, films can be cast in which the complex forms ordered structures [5,6] as has been observed with *atactic* polystyrene sulphonate. So far, studies on polystyrene sulphonate have been restricted to the *atactic* variety of this polymer [9]. Here neutron scattering data obtained in the solution state (in *n*-butanol) and the gel state (nitrobenzene) are presented for two different tacticities of the polymer moiety, *atactic* (aPS) and *isotactic* polystyrene (iPS).

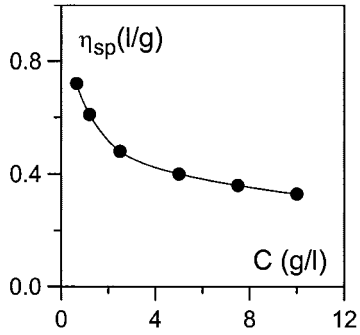

Figure 1. Specific viscosity as a function of concentration for atactic polystyrene sulphonate/CTAB complexes in ethanol. From reference [3].

Experimental

Deuterated styrene was purchased from EURISOTOP and used after proper distillation. Perdeuterated *n-butanol* and perdeuterated nitrobenzene were also purchased from EURISOTOP, and used without further purification. Cetyltrimethylammonium bromide ($CTAB_H$) was obtained from Fluka, hydrogenous *n*-butanol and hydrogenous nitrobenzene were from Aldrich. Perdeuterated atactic polystyrene was synthesized by classical anionic polymerization (M_w= 10^5 with M_w/M_n= 1.26). Perdeuterated isotactic polystyrene was synthesized by Ziegler-Natta catalysis (M_w= $1.2x10^5$ with M_w/M_n = 1.21). These polymers were sulphonated at the same temperature using concentrated sulfuric acid [10]. In what follows these polymers will be designated as $iPSS_D$ (isotactic) and $aPSS_D$ (atactic). Polyelectrolyte/surfactant complexes are prepared through Antonietti et al.'s method [9].

The small-angle neutron scattering experiments were performed on V4, a small-angle camera located at BENSC (Berlin FRG). A selected wavelength of λ_m = 0.6 nm was used with a wavelength distribution function of full width at half maximum, FWHD= $\Delta\lambda/\lambda_m \approx$ 10% (details are available at website http://www.hmi.de/bensc). By moving the sample-detector distance the

available q-range was $0.1 < q$ (nm^{-1}) < 3.0 where $q = (4\pi/\lambda_m) \sin(\theta/2)$, θ being the scattering angle.

Samples were prepared directly in quartz cells from HELLMA of optical paths of 1mm (samples in hydrogenous solvents) or 2 mm (samples in deuterated solvents). Details on the neutron scattering data processing are available in reference 11.

Results and discussion

Solutions in n-butanol

Solutions in *n*-butanol have been prepared with concentrations ranging from C_{comp}= 0.018g/cm^3 to C_{comp}= 0.037g/cm^3. No effect of concentration has been detected. The scattering curves obtained for solutions in *perdeuterated n-butanol* are drawn by means of a Kratky-plot ($q^2I_A(q)$ vs q) in figure 2 for $iPSS_D/CTA_H$ systems for $aPSS_D/CTA_H$ systems. The important outcome is the absence of effect of the polymer tacticity: the molecular structures of either complexes are identical in the explored q-range and concentration range.

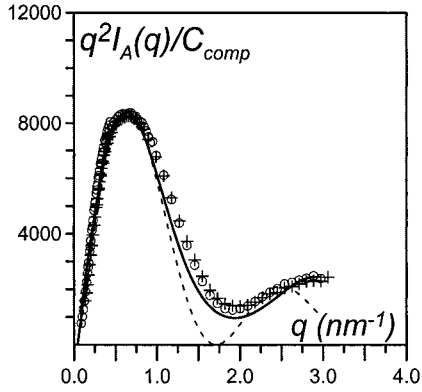

Figure 2. Kratky-plot ($q^2I(q)$ vs q) for solutions in in deuterated n-butanol: $iPSS_D/CTA_H$ complexes (+); $aPSS_D/CTA_H$ complexes (O); C_{comp}= 0.034 g/cm^3.

The scattering curves can be reporduced by using models of rigid cylinders as these systems are expected to take on a bottle-brush structure [12]. The following relation for cylinders of mean length $<L>$ and cross-section radius of gyration r_c [13,14) holds presently:

$$q^2 I_A(q) = C_{comp}\mu_L\left[\frac{\pi q < L > -2}{< L >}\right]\times\varphi(qr_C) \qquad (1)$$

in which μ_L is the mass per unit length, and where $\varphi(qr_c)$ is a function depending on the cylinder cross-section [11].

For $qr_c << 1$ $\varphi(qr_c) \approx 1$ so that μ_L can be determined from the initial slope of the Kratky-plot. One finds μ_L = 8500±2000 g/nmxmole. Considering the molecular weight of the PSS_D/CTA_H repeating unit (474 g/mole), this figure implies about 18±4 repeating units per nanometre. The value of <L>≈ 11 nm is obtained from the intercept q_o with the abscissa ($< L >= 2/\pi q_O$).

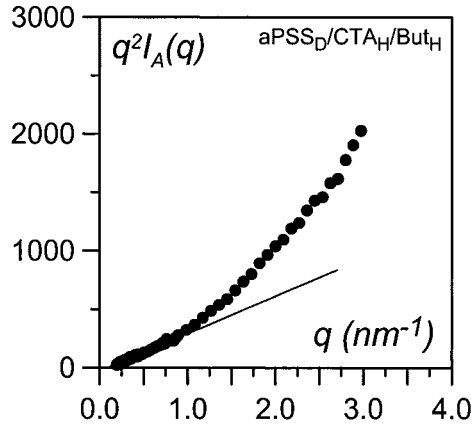

Figure 3. Kratky-plot ($q^2I(q)$ vs q) for $aPSS_D/CTA_H$ complexes in hydrogenous n-butanol; C_{comp}= 0.03 g/cm^3.

The effect of neutron contrast has been examined by dissolving samples of the same polyelectrolyte/surfactant complexes (PSS_D/CTA_H) in *hydrogenous* *n*-butanol. Again, it must be emphasized again that there is no difference whether one uses $iPSS_D$ or $aPSS_D$. Further support to the cylindrical model is obtained as the data reported in figure 3 by means of a Kratky-representation, while also showing a linear variation at small q, eventually display a strong upturn at large q. In the low-q range, where the variation is linear, the mass per unit length is μ_L= 6400±1000 g/nmxmole, a value in good agreement with those measured from solutions in perdeuterated *n*-butanol. The upturn in the large q-range can be accounted for with a cylinder-like structure by introducing a contrast effect in the cross-section scattering. Indeed, the contrast of the polymer moiety and of the CTA wing are of opposite signs (B_{PSSD}= 12.7, B_{CTA}= -0.53) which can lead to the type of effect (see reference 11 for further details).
The cylinder-like structure arises possibly from the formation of a helical-like structure, especially for the case of iPSS complexes. The existence of helices in solutions has also been reported by Ponomarenko et al. with synthetic polypeptides in dilute chloroform solutions [15]. Note that, as shown by Pringle and Schmidt [14], a helical structure scatters as a cylinder for $q<$

$2\pi/P$, where P is the pitch of the helix, which corresponds to the *zeroth order* layer line.

A fit of the data obtained in perdeuterated *n*-butanol has been attempted in the whole q-range by considering one helical form with the best fit yielding γ_1= 0.24 and r_h= 2.1 nm. A better fit is obtained by considering the occurrence of two populations of helices with differing cross-section radius as shown in figure 4. The fit yields **helix 1** r_h= 2.7 nm/γ_1= 0.4 (a), **helix 2** r_h= 1.75 nm/γ_1= 0.33 (b) with X= 0.45 where X is the fraction of helix 1. The existence of two types of helix is suggested by ab-initio calculations performed in the case of isotactic polystyrene, for which it has been shown that *near-tt* arrangements can produce 12_1 and/or 26_1 helices [16,17]. In the case of the 26_1 helix the torsion angles ψ_1 and ψ_2 are of opposite signs which results in the phenyl groups alternating above and beneath the backbone axis. This is reminiscent in some aspect, although to a lesser extent, of the planar zig-zag of syndiotactic polystyrene. In the case of aPS, which consists mainly of syndiotactic tryads, warping of the stablest planar zig-zag form (*tt* conformation) is also likely to give rise to similar helices.

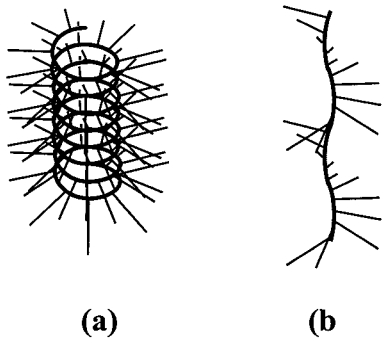

Figure 4. Schematic drawings of the two possible helical structures of the polyelectrolyte moiety considered for the fit in figure 2 (solid line).

Gels from nitrobenzene

In nitrobenzene weak gels are produced both for $iPSS_D/CTA_H$ and for $aPSS_D/CTA_H$ complexes. Typical DSC curves are shown in figure 5. In all cases the melting enthalpies are rather weak ($\Delta H \approx$ 0.2-0.6 J/g for C_{comp}= 0.25 g/cm^3) while the overall DSC traces are similar for $iPSS_D/CTA_H$ gels and $aPSS_D/CTA_H$ gels. The melting temperatures associated with the $aPSS_D/CTA_H$ gels are about 20-30°C higher with respect to those from $iPSS_D/CTA_H$ gels, which implies that the structures formed from the $aPSS_D/CTA_H$ complex are stabler than those formed from the $iPSS_D/CTA_H$ complex.

The scattering curve for $aPSS_D/CTA_H/NbH$ gels differs considerably from that obtained for $iPSS_D/CTA_H/NbH$ gels which is consistent with the DSC findings (figure 6).

In the low-q range ($q< 0.4$ nm^{-1}) the scattering curves obtained on $iPSS_D/CTA_H$ gels in either isotopes of nitrobenzene can be interpreted by means of a model derived by Guenet for arrays of fibrils of density ρ displaying cross-section polydispersity[18]. The cross-section distribution function is of the type $w(r)\sim r^{-\lambda}$ with two cut-off radii r_{min} and r_{max}. The intensity is written in the so-called *transitional regime* [18]:

$$\frac{q^4 I_A(q)}{C} = 4\pi^2\rho\left[A(\lambda)q^{\lambda} - \frac{1}{\lambda r_{\max}^{\lambda}}\right] \Big/ \int_{r_{\min}}^{r_{\max}} w(r)dr \qquad (2)$$

Here, $\lambda \approx 1$ and relation 2 reduces to:

$$\frac{q^4 I_A(q)}{C} = \frac{2\pi^2\rho}{Log(r_{\max}/r_{\min})} \times \left[q - \frac{2}{\pi r_{\max}}\right] \qquad (3)$$

A linear behaviour is therefore expected whose intercept q_o with the *q-axis* ($q_O = 2/\pi r_{\max}$) allows one to derive r_{max}= 9.2±0.3 nm.

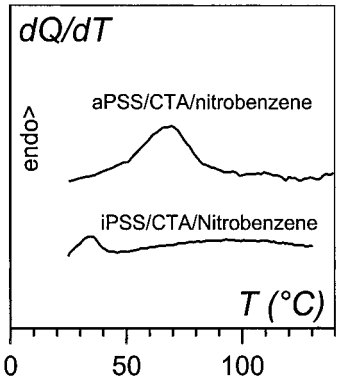

Figure 5. DSC traces obtained at 10°C/m for gels prepared in nitrobenzene: upper curve aPSS/CTA/nitrobenzene gels, lower iPSS/CTA/nitrobenzene gels. C_{comp}= 0.2 g/cm^3.

In principle, the *Porod regime* ($1/q^4$) should be observed after the *transitional regime*. This regime is virtually absent and obliterated by a terminal regime which differs whether the scattering curves have been obtained from gels in hydrogenous nitrobenzene or perdeuterated nitrobenzene (further details in reference 11).

For $aPSS_D/CTA_H/NbH$ gels there are maxima in a $q^4 I_A(q)$ vs q representation that may suggest a much lower cross-section polydispersity of the fibrils. The low-q domain ($q< 0.4$ nm^{-1}) can be fitted with a relation for a straight fibril of infinite length and cross-section radius r_c :

$$q^4 I_A(q) = C_{comp}\mu_L \pi q \times \frac{4J_1^2(qr_c)}{r_c^2} \quad (4)$$

The fit yields r_c= 12.7 nm. That the oscillations are damped at larger q-values may come from a slight polydispersity in cross-section radius.

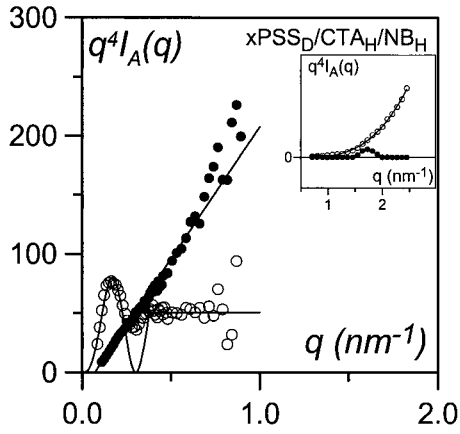

Figure 6. Low-q domain for the intensity scattered by gels in hydrogenous nitrobenzene in a $q^4I(q)$ vs q representation. (O) $aPSS_D/CTA_H$, C_{comp}= 0.028 g/cm^3 (•) $iPSS_D/CTA_H$, C_{comp}= 0.026 g/cm^3. Solid lines are fits (see text for details). Inset: scattering at larger q which evidences the occurrence of a maximum for $aPSS_D/CTA_H$ complexes.

The outcomes from these neutron scattering experiments is consistent with the thermal properties. A lesser cross-section polydispersity together with a larger fibril's cross-section is consistent with a higher melting temperature for $aPSS_D/CTA_H$/Nitrobenzene gels with respect to $iPSS_D/CTA_H$/Nitrobenzene gels.

Of further interest are the scattering curves in the high-q range in hydrogenous nitrobenzene (NbH) shown in inset of figure 5. The scattering intensity for $iPSS_D/CTA_H$/NbH gels increases monotonously while that for $aPSS_D/CTA_H$/NbH gels is virtually flat and displays a maximum at q= 1.75 nm^{-1}. This maximum is likely to arise from a lamellar organisation in the fibrils as was reported by Antonietti and coworkers [9]. Conversely, the absence of maximum in $iPSS_D/CTA_H$/NbH gels suggests that the helical chains simply pack with a very short-range order.

Concluding remarks

The results highlight the absence of effect of the polymer moiety tacticity on the molecular structure of polystyrene sulphonates/CTAB complexes in solutions. Evidently, the surfactant determines the molecular structure. Conversely, polymer tacticity influences the organization of the gel state. While lamellar structure seems to occur for complexes prepared from atactic polystyrene sulphonate, a much poorer order seems to set in for gels produced from isotactic polystyrene sulphonate.

[1] Hayagawa, K.; Kwak, J.C. *J. Phys. Chem.* **1982** *86* 3866
[2] Goddard, E.D. *Colloids Surf.* **1986** *19* 301
[3] Antonietti, M.; Burger, C.; Thünemann, A. *Trends Polym. Sci.* **1997** *5* 262 and references therein
[4] Ober, C.K.; Wegner, G. *Adv. Mater.* **1997** 9 17 and references therein
[5] Harada, A.; Nozakura, S. *Polym. Bull.* **1984** *11* 175
[6] Taguchi, K.; Yano, S.; Hiratani, K.; Minoura, N.; Okahata, Y. *Macromolecules* **1988** *21* 3336
[7] Ciferri, A. *Macromol. Chem. Phys.* **1994** *195* 457
[8] Thalberg, K. and Lindman, B., *Surfactants in Solution* Vol. 11, Eds. Mittal, K.L. and Shah, D., Pleneum Press, N.Y **1991**.
[9] Antonietti, M.; Conrad, J.; Thünemann, A. *Macromolecules* **1994** *27* 6007
[10] Vink, H. *Makromol. Chem.* **1981** *182* 279
[11] Ray, B.; ElHasri, S.; Guenet, J.M. *Eur. Phys. J. E* **2003** *11* 315
[12] Fredrickson, G.H. *Macromolecules* **1993** *26* 2825
[13] Fournet, G. *Bull. Soc. Franç. Minér. Crist.* **1951** *74* 39
[14] Pringle, O.A.; Schmidt, P.W. *J. Appl. Crystallogr.* **1971** *4* 290
[15] Ponomarenko, E.A.; Tirrell, D.A.; MacKnight, W.J. *Macromolecules* **1996** *29* 8751
[16] Beck, L.; Hägele, P.C. *Colloid Polym. Sci.* **1976** *254* 228
[17] Atkins, E.D.T.; Isaac, D.H.; Keller, A. *J. Polym. Sci. Polym. Phys. Ed.* **1980** *18* 71
[18] Guenet, J.M. *J. Phys. II* **1994** *4* 1077